Available online at www.sciencedirect.com
ScienceDirect
Remote Sensing of Environment 104 (2006) 62–73
Remote Sensing of Environment
www.elsevier.com/locate/rse

Mapping shrub abundance in desert grasslands using geometric-optical modeling and multi-angle remote sensing with CHRIS/Proba

Mark Chopping [a,*], Lihong Su [a], Andrea Laliberte [b], Albert Rango [b], Debra P.C. Peters [b], Naushad Kollikkathara [a]

[a] Earth and Environmental Studies, Montclair State University, Montclair, NJ 07043, USA
[b] USDA, ARS Jornada Experimental Range, Box 30003, MSC3JRN, NMSU, Las Cruces, NM 88003, USA

Received 29 January 2006; received in revised form 24 April 2006; accepted 29 April 2006

Abstract

This work examines the application of a geometric-optical canopy reflectance model to provide measures of woody shrub abundance in desert grasslands at the landscape scale. The approach is through inversion of the non-linear simple geometric model (SGM) against 631 nm multi-angle reflectance data from the Compact High Resolution Imaging Spectrometer (CHRIS) flown on the European Space Agency's Project for On-Board Autonomy (Proba) satellite. Separation of background and upper canopy contributions was effected by a linear scaling of the parameters of the Walthall bidirectional reflectance distribution function model with the weights of a kernel-driven model. The relationship was calibrated against a small number of sample locations with highly contrasting background/upper canopy configurations, before application over an area of about 25 km^2. The results show that with some assumptions, the multi-angle remote sensing signal from CHRIS/Proba can be explained in terms of a combined soil–understory background response and woody shrub cover and exploited to map this important structural attribute of desert grasslands.

Keywords: Canopy reflectance; Geometric-optical; Modeling; Multi-angle remote sensing; Semi-arid environments; Dessert grasslands; Woody shrub encroachment

1. Introduction

Arid and semi-arid lands, including desert, scrubland, grassland and savanna, cover about 40%, or an estimated 58.5 million km^2, of the terrestrial surface (Atjay et al., 1979). Vast areas within these biomes, including a large proportion of the southwestern USA, have experienced a dramatic increase in the abundance of woody shrub vegetation over the last century, replacing a former relatively continuous cover of grasses. This has resulted in changes to hydrological and biogeochemical cycles as well as profound impacts on the ecology and economic value of the land at local to regional scales (contraction of the livestock industry) and on the surface radiation budget at regional to global scales (the albedo of shrub-dominated land is much higher as bright soils are more exposed). Scientists are thus interested in methods for assessing the condition of the land for the purposes of furthering management and conservation goals, for predicting ecosystem response to future disturbance regimes, and for measuring fluxes of energy and materials at the lower boundary. Of particular interest to ecologists is the mapping of upper canopy (large shrub) horizontal distributions and gap fraction which is related to fetch lengths and is important in dynamic "gap" models of landscape-scale processes, such as seed dispersal, the potential for the spread of fire, and feedbacks between vegetation, hydrologic and soil processes. Gap models are extremely useful in predicting plant- and species-level responses and interactions under a variety of environmental conditions but are limited in the spatial extent that can be simulated as a result of the small plot size on which they operate and the detailed processes included (Peters & Herrick, 2001). They require at minimum information on dominant plant type: the ability to map shrub abundance, number density and size distributions is therefore critical if these models are to be implemented over large areas.

* Corresponding author.
E-mail addresses: chopping@pegasus.montclair.edu (M. Chopping), su@pegasus.montclair.edu (L. Su), alaliber@jornada-mail.nmsu.edu (A. Laliberte), alrango@nmsu.edu (A. Rango), kollikkathn1@mail.montclair.edu (N. Kollikkathara).

0034-4257/$ - see front matter © 2006 Elsevier Inc. All rights reserved.
doi:10.1016/j.rse.2006.04.022

Since the large extent, limited accessibility and surface heterogeneity of deserts prohibits the use of ground survey in monitoring, remote sensing is the only means of obtaining geographically comprehensive measurements. Remote sensing from Earth observation satellites is a powerful tool that has been used to examine trends in dryland degradation since the 1980s, with varying degrees of success. Remote sensing of vegetation in drylands presents a number of specific challenges, not least because of the very low levels of vegetation cover and highly discontinuous canopies. The most widely used method for assessing vegetation abundance, photosynthetic activity and biomass – spectral vegetation indices calculated as ratios of red/near-infrared (NIR) reflectance – are not as useful in arid environments as elsewhere since they are based on the observed absorption of red light by leaf pigments and the assumption of a relatively NIR-dark soil. However, dryland mineral soils are bright in the NIR, rendering such indices ineffective (Calvão & Palmeirim, 2004; Ni & Li, 2000; Rahman & Gamon, 2004; Ray, 1995), even though some of these indices attempt to compensate for changes in soil color, e.g. the Soil-Adjusted Vegetation Index (SAVI; Huete, 1988) and the Modified SAVI (Qi et al., 1994). If the surface is conceptually divided into upper canopy and lower canopy+soil, then soil spectral response is not the most important control on brightness and variations in understory cover have a more profound impact. Similar constraints limit the utility of multispectral imaging in most regions of the solar spectrum: the reflectance response is highly correlated across most of this wavelength region.

Recent developments in remote sensing technology such as imaging spectroscopy and very high resolution imaging, which are proving very useful in other environments, also have limitations when used in arid regions. It has been shown from first principles that the ability of imaging spectroscopy to provide a spectral vegetation signal is limited when fractional cover is below 0.3 (Okin et al., 2001), although some success has been reported in unmixing of spectra to estimate the fractional covers of soil, photosynthetic and non-photosynthetic vegetation (Asner et al., 2003). Very high resolution imaging by the latest generation of commercial imagers with meter or sub-meter ground sampling distances (IKONOS, QuickBird) could provide much of the required canopy information over large areas — but the cost of data for a mapping effort for a single year would be high and data volumes would be huge and relatively unmanageable even with today's fast, capacious computers. Scientists – ecologists, hydrologists, biogeographers and meteorologists – do not generally possess the financial or computing resources to tackle such projects and most fall back on the tried and trusted but ultimately limited approach of using a spectral vegetation index as the major source of information. More importantly, process models must be driven with parameters obtained at regular intervals, typically from daily to monthly frequencies.

An alternative approach is to use multi-angle moderate field-of-view data with techniques designed to exploit the directional signal by either empirical metrics (e.g., ratios of image values acquired at differing viewing orientations) or by modeling the changing reflectance with respect to illumination and viewing angle; i.e., modeling the bidirectional reflectance distribution function (BRDF). In arid environments with very low leaf area per unit area, the main physical phenomenon underlying observed changes is shadowing of the background by plants. Models which explain changes in the spectral reflectance of a partly vegetated surface with respect to illumination and viewing angles and the physical structure and optical properties of canopy elements have been developed. These models attempt to describe and may partly explain the surface BRDF. Geometric-optical (GO) models are one class of such models and these treat the surface as an assemblage of discrete, identical, and relatively large geometric objects placed in a Poisson distribution above an underlying surface (Chen et al., 2000; Li & Strahler, 1992) which is frequently considered Lambertian but may also be characterized by its own BRDF (Ni & Li, 2000). The remotely sensed observation is modeled as a linear combination of contributions from viewed sunlit and shaded components, with each contribution a product of component reflectance and the fraction of the sensor's field of view occupied by the component.

GO models have been used successfully to estimate forest canopy metrics (Gemmell, 2000; Pilger et al., 2002; Scarth & Phinn, 2000) and appear to have great potential (Chen et al., 2000). The Li–Strahler geometric-optical (GO) model (Li & Strahler, 1992) is one of the best known of this type of model and been found to perform well in forest environments (Schaaf et al., 1995). Similar models have also been used in theoretical and validation studies in desert grasslands and shrublands (Chopping et al., 2003, 2004a,b; Ni & Li, 2000; Qin & Gerstl, 2000). In spite of their successful application in forests, GO models have not been used to estimate shrub canopy parameters in drylands at landscape scales. This may be because in forest environments the background makes a small contribution to the signal relative to tree crowns and is often composed of a fairly homogeneous understory of relatively high cover with spectral reflectance characteristics similar to leaves of trees and on dark organic soils. Several workers have noted that even in forest environments the understory can present problems for GO modeling (Bowyer et al., 2001; Gemmell, 2000). In arid environments the background of mineral soils, litter and mixed understory plant cover of grasses, sub-shrubs and annuals is much more important in governing brightness than in forests. Background (soil plus understory) fractional cover usually exceeds 0.7 and the high brightness relative to leaves, stalks and branches of large plants reduces the vegetation-specific information content of the signal.

More importantly for GO modeling, all types of backgrounds – even bare soils – exhibit quite strong reflectance anisotropy which must be accounted for separately from the larger scale geometric effects of large plants (shrubs). This was recognized in Ni and Li (2000), where a background BRDF was injected into the canopy reflectance model. Using a static background BRDF would work well in situations where the background composition does not vary importantly from place to place. Herein lies the first major difficulty in applying GO models to measuring canopy parameters in arid shrublands: in these environments the soil–understory background composition and anisotropy vary substantially from location to location on scales of a few tens of meters. In order to separate the effects of the upper canopy (shrubs) and the

background an alternative to adopting a static background BRDF must be employed.

A second major problem is that GO models are formulated so that plant number density and cover appear as a single internal parameter. The same proportions of viewed and illuminated and shaded crown and background are obtained for either a small number of large plants or a large number of small plants, keeping total plant cover constant. This means that even if we were able to successfully decompose the remotely sensed signal into upper canopy and background contributions, we would still only be able to obtain a measure of upper canopy cover. For many applications this information may be sufficient; however we would like to know more about the canopy. This problem has been noted by workers and the need to provide additional *a priori* information has been recognized (Combal et al., 2002; Li et al., 2002; Weiss et al., 2000).

The major challenge addressed in this work is therefore how to use a GO model to separate the upper canopy and background contributions. A second problem, how to decompose upper canopy cover into plant size and number density, is addressed in a separate study. Neither of these problems is trivial but only if the first is adequately resolved can GO models be exploited effectively in arid grasslands.

2. Method

2.1. The study area: the USDA, ARS Jornada Experimental Range

The USDA, ARS, Jornada Experimental Range lies about 37 km north of Las Cruces, New Mexico (32.5°N, 106.8°W) and is 1 of the 22 core sites worldwide selected for the exploitation of data from the CHRIS instrument on Proba, launched on October 22, 2001 (Rango et al., 1998) (Fig. 1). The Jornada Experimental Range is located in the northern part of the Chihuahuan Desert between the Rio Grande floodplain (elevation 1186 m) on the west and the crest of the San Andres mountains (2833 m) on the east. It is located at the southern end of a hydrologically closed basin and is characterized by a complex system of alluvial fans (bajadas) and ephemeral playa lakes. Much of the basin is dominated by coarse-textured aeolian and fluvial sediments from the Rio Grande. Mean elevation is about 1350 m. Climate is arid to semiarid: long-term (1916–1995) mean annual precipitation was 249 mm/year (S.D. = 87) and mean monthly temperatures ranged from 3.8 °C in January to 26.1 °C in July. The Jornada is characterized by a monsoonal pattern in precipitation with more than half annual rainfall occurring in July–September. Vegetation is classified as desert grassland and shrub density has increased dramatically since the 1880s and is continuing to do so (Gibbens et al., 1992). *Prosopis glandulosa* (honey mesquite) is now a major dominant on sandy soils where *Gutierrezia sarothrae* (broom snakeweed) and *Yucca elata* (soaptree yucca) are also abundant. Uplands are dominated by the perennial C_4 grass, *Bouteloua eriopoda* (black grama) occurring on sandy loams to loamy soils and are often dominated by the C_3 shrub, *Larrea tridentata* (creosotebush). Other grasses, succulents, shrubs, and forbs account for the remainder of plant cover.

2.2. CHRIS multi-angle data

The CHRIS sensor developed by Sira Electro-Optics Ltd. (UK) produces imagery in up to 62 spectral channels in the range 415–1050 nm with a spectral resolution of 5–12 nm. It is highly configurable in terms of both spectral channels and spatial resolution (European Space Agency 1999). Calibrated spectral radiance images in 18 bands from 442 nm to 1019 nm (CHRIS Mode 3 — Land Channels) have been obtained over desert grasslands in the Jornada Experimental Range since the launch of

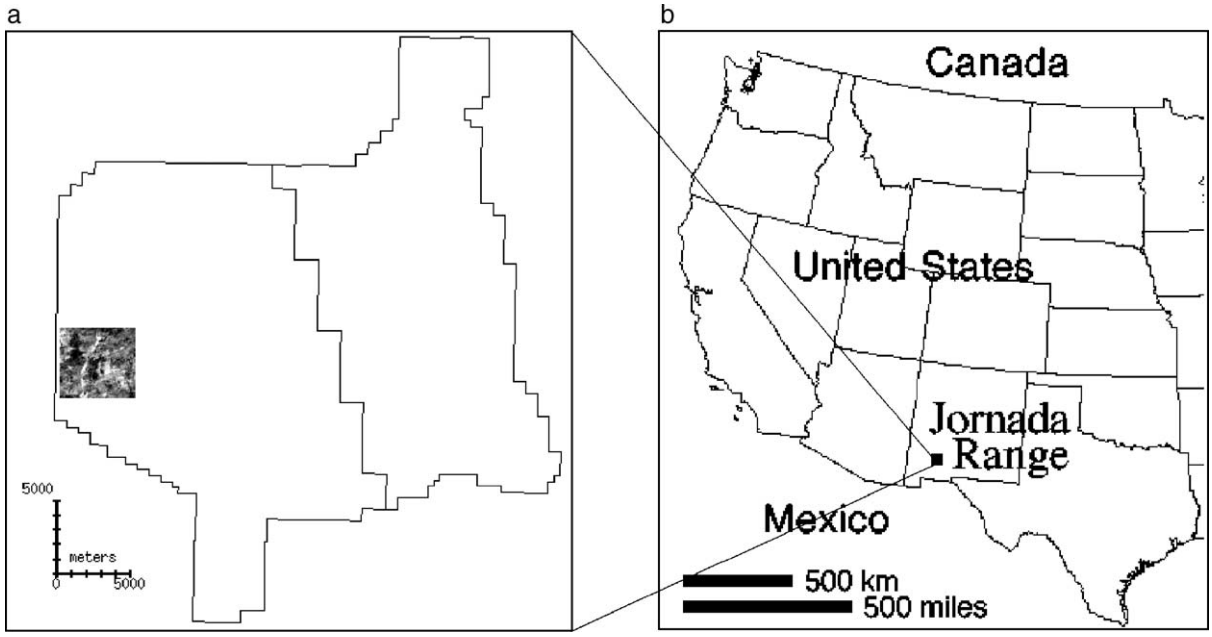

Fig. 1. (a) The location of the CHRIS scene in relation to the USDA, ARS Jornada Experimental Range. (b) The location of the Range in New Mexico, USA.

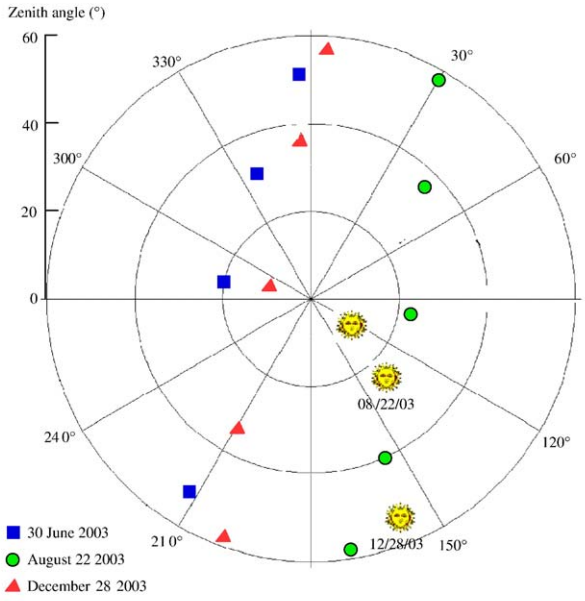

F/B	IMAGE#	SZA (°)	SAA (°)	VZA (°)	VAA (°)	RAA (°)
F	21	26.30	138.47	55.67	29.90	108.57
F	1F	26.18	138.85	38.27	46.33	92.52
B	1E	26.07	139.22	24.35	105.27	33.95
B	20	25.95	139.60	40.53	158.53	18.93
B	22	25.85	139.98	57.85	173.37	33.39

Fig. 2. CHRIS/Proba angular sampling over the Jornada Range at three times of year. The table shows the angular sampling for the images used in this study; B and F indicate back- and forward-scattering directions, respectively; SZA, SAA, VZA, VAA, and RAA are solar zenith, solar azimuth, view zenith, view azimuth, and relative azimuth angles, respectively. Image #22 was not used in this study as the overlap area was too small.

Proba in October 2001, providing up to five angular looks in the space of a few minutes via tilting and nodding of the satellite. Mode 3 provides a nominal ground sampling distance of ~17 m with a full swath. A CHRIS image set from August 22, 2003 was selected for this study; this date is towards the end of the wet growing season with maximum green foliage. The areas imaged by CHRIS encompass a variety of plant communities and topoedaphic conditions, including black grama grassland, grass–shrub transition, mesquite- and creosotebush-dominated shrubland, areas infested with broom snakeweed, areas of sand entrainment and deposition, experimental plots, and swales. The images were co-located using sets of >30 ground control points based on features such as road intersections, pits, and swales. A 1 m IKONOS panchromatic image was used as the reference. The images were then resampled to a 25 m grid on a UTM map projection using low-order polynomial transforms with a nearest-neighbor rule. The absolute root mean square error (RMSE) at the control points was at all times <3 m and the match between transformed and reference images was carefully checked across the images and not just at control point locations. Image acquisition times were used with orbital ephemeris and the Xephem software package to obtain the satellite zenith and azimuth angles. The angular sampling for typical CHRIS overpasses is shown in Fig. 2. The August 22 set was acquired with a 26° solar zenith angle and provides one look close to the solar principal plane and three close to the perpendicular plane. Viewing zeniths range from 24° to 55°. A high quality December 28, 2003 CHRIS data set providing a superior angular sampling closer to the principal plane and a large overlap region with five looks was also processed the same way; however in the winter months mesquite shrubs are leafless and cannot be treated as spheroids, a prerequisite for treatment with GO models.

Surface spectral reflectance estimates were calculated using 6S v4.2 (Vermote et al., 1997) for all Mode 3 bands and assuming a desert aerosol type. Meteorological data indicated a visibility of 16.1 km for August and December overpasses, from which an optical thickness at 550 nm of 0.3 was estimated. Forward-scattering reflectance values are considerably lower than near-nadir values for all wavelengths as a result of the increased visibility of shadows cast by vegetation and soil roughness elements (Fig. 3). Similarly, back-scattering reflectance values are higher than those close to nadir since there is a greater degree of shadow-hiding.

2.3. Simple geometric model

The non-linear simple geometric model (SGM; Chopping et al., 2003, 2004a, 2005) was adopted for this study. The SGM was developed by relaxing some important assumptions made by kernel-driven BRDF models and is intended for the purposes of inversion against multi-angle data. As with kernel-driven models, the SGM assumes potential contributions from both geometric-optical and volume scattering effects and is formulated as (Eq. (1)):

$$R = G_{\text{Walthall}}(\vartheta_i, \vartheta_v, \varphi)\cdot k_G(\vartheta_i, \vartheta_v, \varphi) + C_{\text{Ross}}(\vartheta_i, \vartheta_v, \varphi)\cdot k_C(\vartheta_i, \vartheta_v, \varphi) \quad (1)$$

where the subscripts i and v, refer to illumination and viewing angles; ϑ_i, ϑ_v and φ are the solar zenith, view zenith and relative azimuth angles, respectively; k_G and k_C are the

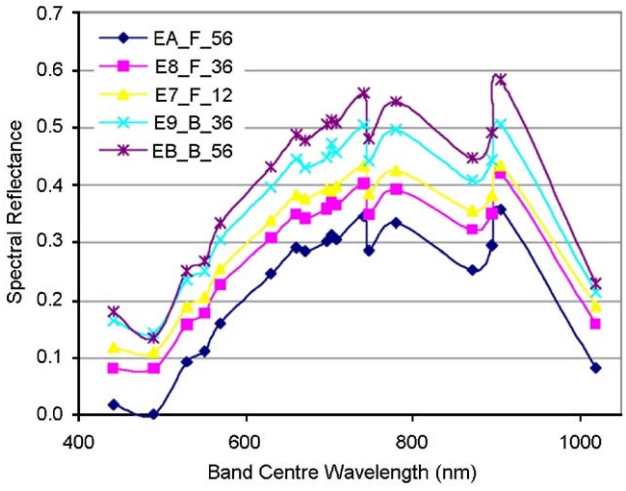

Fig. 3. Example CHRIS spectra (12/28/03) for a bright target in the Jornada Experimental Range. The solar zenith angle is 57°. The legend shows the 2-character scene code, viewing in the (F)orward or (B)ack-scattering hemisphere, and view zenith angle. Lines are smoothed for clarity only. Note the higher error in the shorter wavelengths.

Table 1
Percent cover and calculated fractions of viewed and sunlit background and crown (k_G and k_C, respectively) and shaded components (K_Z+T) at nadir viewing for seven sites

Plot #	Shrub Cover (%)		k_G	k_C	K_Z+t
	Measured [a]	Modeled			
1	5.9	6.1	0.93	0.03	0.04
2	5.5	4.8	0.94	0.02	0.04
3	10.9	11.6	0.81	0.06	0.14
4	5.1	8.6	0.88	0.04	0.08
5	12.2	8.3	0.87	0.04	0.09
6	13.0	12.8	0.77	0.06	0.16
7	15.1	11.9	0.80	0.06	0.14

[a] Measured by counting 1 m pixels in the May 23, 2001 IKONOS panchromatic image.

calculated proportions of sunlit and viewed background and crown, respectively (Table 1); G_{Walthall} is the calibrated Walthall model (Walthall et al., 1985); and C_{Ross} is the simplified Ross turbid medium approximation for optically-thin or thick plane parallel canopies (Ross, 1981). k_G and k_C are calculated exactly via Boolean geometry for the principal (PP) and perpendicular (CPP) planes and approximated away from these (Wanner et al., 1995). The parameters are shrub density, crown radius, shape and center height, and leaf area index. This model is not a physical model as the radiative properties of the surface are not handled explicitly; for example, the effects of diffuse irradiance are ignored and all shadows are considered completely dark, as in Li–Ross kernel driven BRDF models. However the SGM has provided good results when tested against a radiosity-based model calibrated with detailed ground measurements and against multi-angle observations from the air (Chopping et al., 2003, 2004a), and provides some advantages over the kernel driven models. The most important difference between kernel-driven models and the SGM is that the assumption that the signatures of illuminated crown and background are identical is relaxed in the latter.

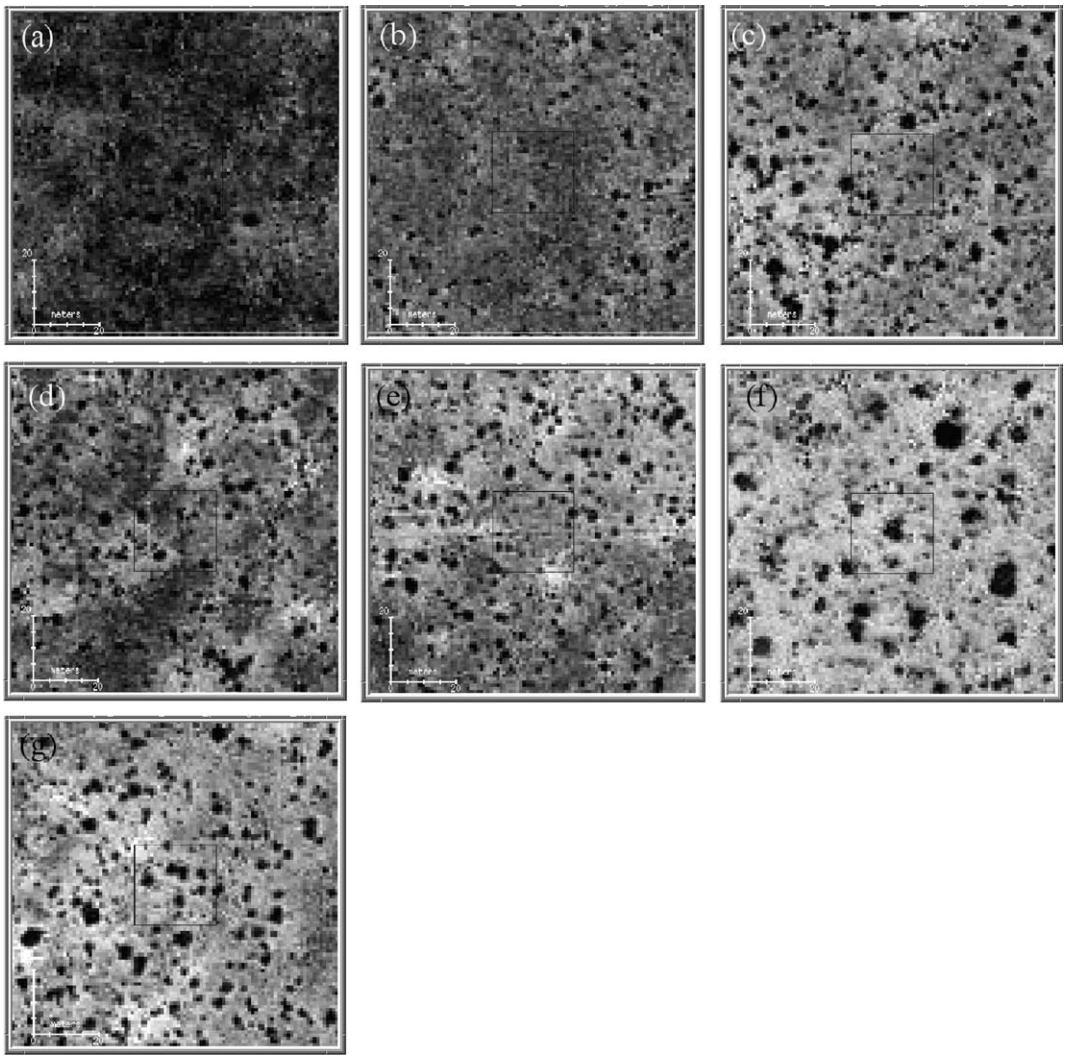

Fig. 4. IKONOS 1 m panchromatic image chips showing contrasting upper canopy and background configurations. The dark blobs are mostly honey mesquite shrubs. Gray areas are mixtures of soil, black grama grass, broom snakeweed and a small proportion of other low plants. Boxes show the areas corresponding to CHRIS observations mapped at 25 m^2.

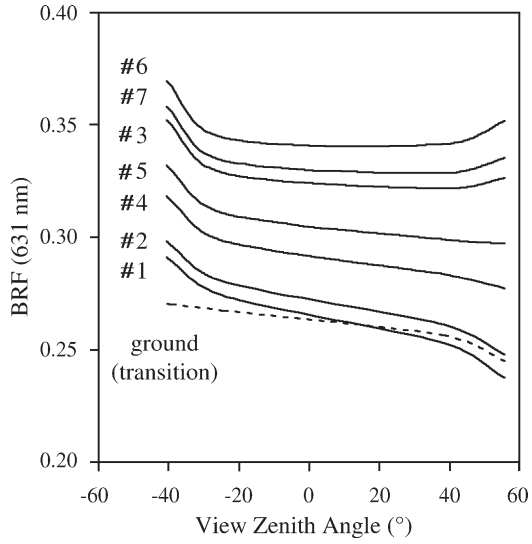

Fig. 5. Initial attempts at scaling the Walthall model with CHRIS near-nadir brightness (SZA=26°, VZA=24°, RAA=33°) for the seven test plots (solid lines; #1–7 are for the plots shown as (a) through (g) in Fig. 4). The dotted line is for a ground-measured sand BRDF at the transition site (Betty Walter-Shea/ Grassland PROVE Experiment).

2.4. Obtaining the spatially dynamic background contribution

As noted above, the major challenge for the practical application of GO models is to separate the upper canopy and background contributions. In previous SGM inversions using multi-angle images from the air the Walthall background sub-model was adjusted against ground-based angular radiometry close to the limited (300–600 m^2) areas mapped to obtain static background BRDFs for grassland and sand. The SGM was originally conceived with the division of the surface into soil, understory and upper canopy elements; however this approach is not practical over large areas in an environment where the soil and understory fractions vary importantly and the canopy is highly discontinuous. Even in this desert large areas of absolutely bare soil are only apparent in isolated locations (e.g., roads and areas with high deposition of wind-borne soil), so it is difficult to obtain a pure soil BRDF, even if this were desirable. Treating the surface as divided discretely into soil background and vegetation components is sub-optimal because fractional shrub cover or other parameters retrieved will contain information on both upper canopy and understory vegetation.

It is more appropriate to instead attempt to model the surface as a background composed of a combined soil–understory complex on which there are a varying number of larger plants. This is still conceptually different from the real world situation because the upper canopy can only be modeled as a varying number of plants of a single size and shape; there is no mechanism for modeling size and shape distributions to account for large plants of different species and stages of maturity. However, the approach is acceptable as a first approximation and is more valid than adopting a static soil–understory BRDF. The background BRDF must thus be characterized for each location and for the angular configurations of interest, using CHRIS data.

In a first attempt at inverting the SGM with CHRIS data the Walthall soil–understory sub-model was driven by CHRIS multi-angle observations. Contiguous areas of 25 m^2 were selected and the sub-model parameters were scaled according to brightness in the CHRIS near-nadir image (Chopping et al., 2004b). This is based on the assumption that brightness in remotely sensed scenes with a ground sampling distance greater than a few meters is controlled mainly by the understory rather than by large plants, with the exception of swales. It can be viewed as a means of injecting *a priori* information into the inversion problem. Examination of aerial photography and very high resolution panchromatic imagery indicates that this assumption might be reasonable (Fig. 4). The separation is challenging because we not only want to estimate shrub cover,

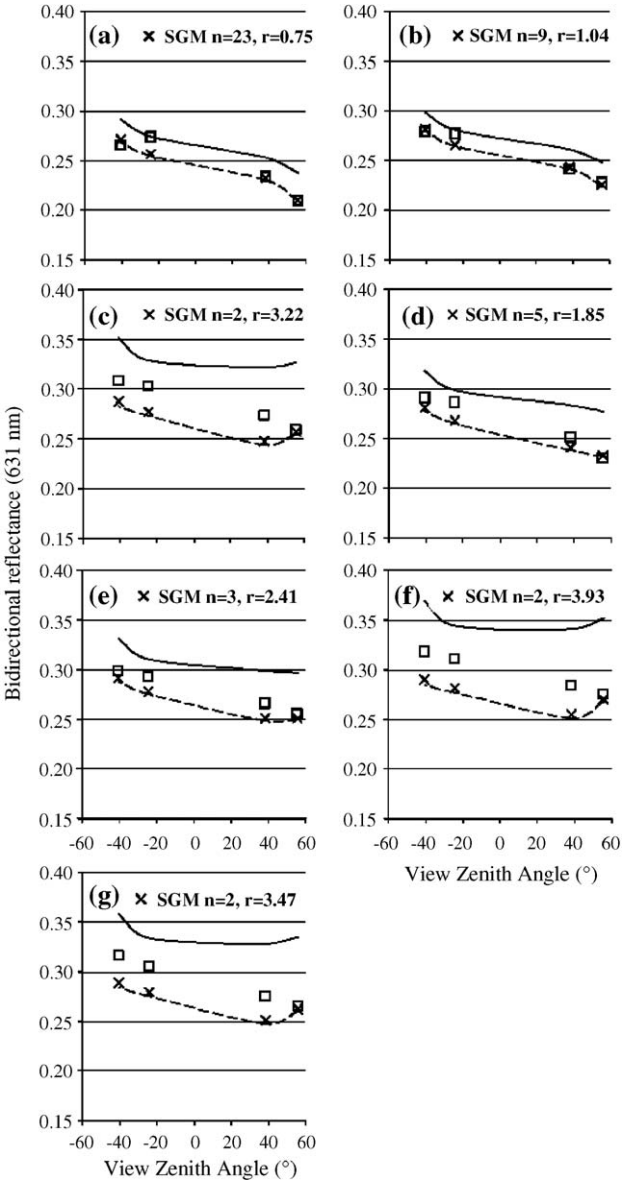

Fig. 6. Walthall model reflectance values for 100% illuminated and viewed background (solid line); ditto, weighted for the GO-calculated proportion of illuminated and viewed background (dotted line), CHRIS reflectance values (squares), and modeled with SGM (crosses). n=number of shrubs; r=mean shrub radius.

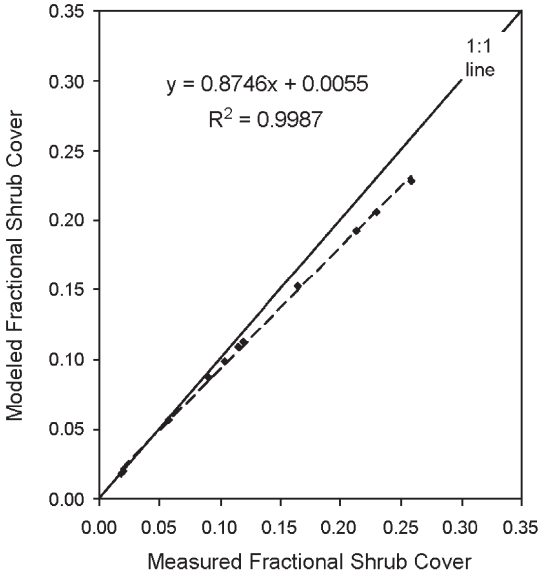

Fig. 7. Modeled woody shrub cover vs. cover estimated from IKONOS panchromatic imagery for the calibration data set. These results were obtained by using the optimal Walthall model coefficients and adjusting shrub number density and mean radius against CHRIS data sets, starting with the shrub density and mean radius set to arbitrary values of 0.01, and mean mid-crown height and crown shape set to 2.0 and 0.2, respectively.

number density and size over bright soil backgrounds but also over mixed grass and sub-shrub understories of varying brightness. This was a first attempt to separate the soil–understory background and the upper canopy contribution; however, as noted above it is inappropriate to use a winter scene for GO modeling and the scaling coefficients used were not accurate. The results were poor – the cover maps retrieved were highly inaccurate – mainly because the SGM inversions are extremely sensitive to the estimates of the background contribution and the need for further refinement of the technique was apparent. To refine the calibration of the background sub-model, coefficients were obtained by selecting two areas with contrasting upper canopy and background configurations; setting SGM shrub number density and radius parameters according to the observed configurations corresponding to the mapped CHRIS observations (e.g., inside the boxes in Fig. 4); and adjusting the Walthall model parameters so that the SGM matches observations using an optimization algorithm. Shrub number density and mean radius per 25 m^2 were obtained by setting statistical thresholds on 25 m^2 subsets of a 1 m May 2003 IKONOS panchromatic image using an algorithm developed with medical imaging software (the NIH Image package distributed by the US National Institutes of Health). A linear scaling with near-nadir CHRIS brightness was assumed and slopes and intercepts were calculated for use over the landscape. Note that scaling the parameters in this way represents an attempt to adjust for both the magnitude (brightness) and shape (anisotropy) of the background (Fig. 5). We thus attempted to account for the background by making the assumption that the background accounts for the bulk brightness, rather than the larger plants. Since we cannot easily model the background mixture we made use of this assumption and estimated a Walthall BRDF model with coefficients scaled according to near-nadir brightness: the remaining contribution required to match the modeled reflectance to multi-angle observations should be from the effects of large shrubs (reducing brightness). However, the underlying assumption may not be valid. The third attempt to calibrate coefficients allowing estimates of the background contribution was effected using the same optimization technique but for a larger number of locations and a wider range of canopy-background configurations. Again, measured shrub number density and mean radius parameters were used to obtain optimal Walthall model parameters; however this time the red wavelength weights of a kernel driven Li–Ross model (isotropic-LiSparse-RossThin kernels) were used to predict the Walthall background model coefficients. This method was used for all subsequent work; the kernel weights provide superior information to the regression since three parameters are available. Even though these are not necessarily uncorrelated they do encapsulate information on the 3-D structure of the canopy–soil complex (Gao et al., 2003).

The effectiveness of these methods in allowing separation between background and shrub contributions was evaluated by examining the behavior of the SGM for a number of selected 25 m^2 locations of dramatically different canopy and background configurations (Fig. 6). It can be seen that the match between modeled and observed values is not always precise; however the number and density follow the expected trend with the exception of the dark, dense background with a large mesquite upper canopy ((a) in Figs. 4 and 6). When the "optimal" estimates of the background contribution are used (with calibration of the Walthall model based on Li–Ross model kernel weights), the modeled shrub cover is very close to that observed, indicating that error in

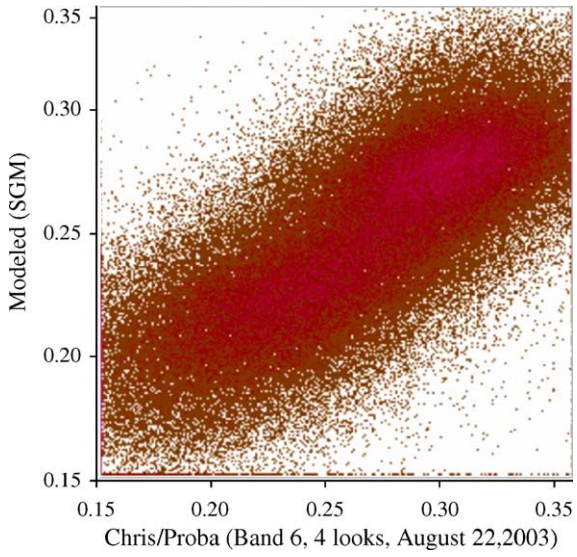

Fig. 8. CHRIS/Proba estimated surface bidirectional reflectance (red wavelengths) *vs*. surface bidirectional reflectance modeled using SGM driven with IKONOS-derived shrub statistics and Walthall model backgrounds estimated from Li-Ross model kernel weights. R^2=0.74, RMSE=0.021, y=0.8154x+0.0478, N=155,736. (For interpretation of the references to colour in this figure legend, the reader is referred to the web version of this article.)

retrieving shrub cover is almost entirely owing to inaccuracies in estimating the background contribution (Fig. 7).

2.5. Simulation of CHRIS imagery

The SGM was driven using spatially dynamic background contributions from the calibrated Walthall model and IKONOS-derived shrub statistics (mean radius, number density), with the *h*/*b* and *b*/*r* parameters set at fixed values of 2.00 (low; typical) and 0.2 (very oblate crowns). Some differences might be expected as a result of the different acquisition times of the reference and CHRIS data: the IKONOS 1 m panchromatic image from which shrub statistics were extracted was acquired in May 2003 whereas the CHRIS scene was acquired in August of the same year.

2.6. SGM model inversions

For each mapped 25 m^2 location the SGM was adjusted against the CHRIS data (38,934 locations) by means of numerical optimization methods (forward differencing was used for estimates of partial derivatives of the objective function and a Newton search method was used at each iteration to decide which direction to pursue in the parameter space). The objective function was min(absolute RMSE) with no weighting

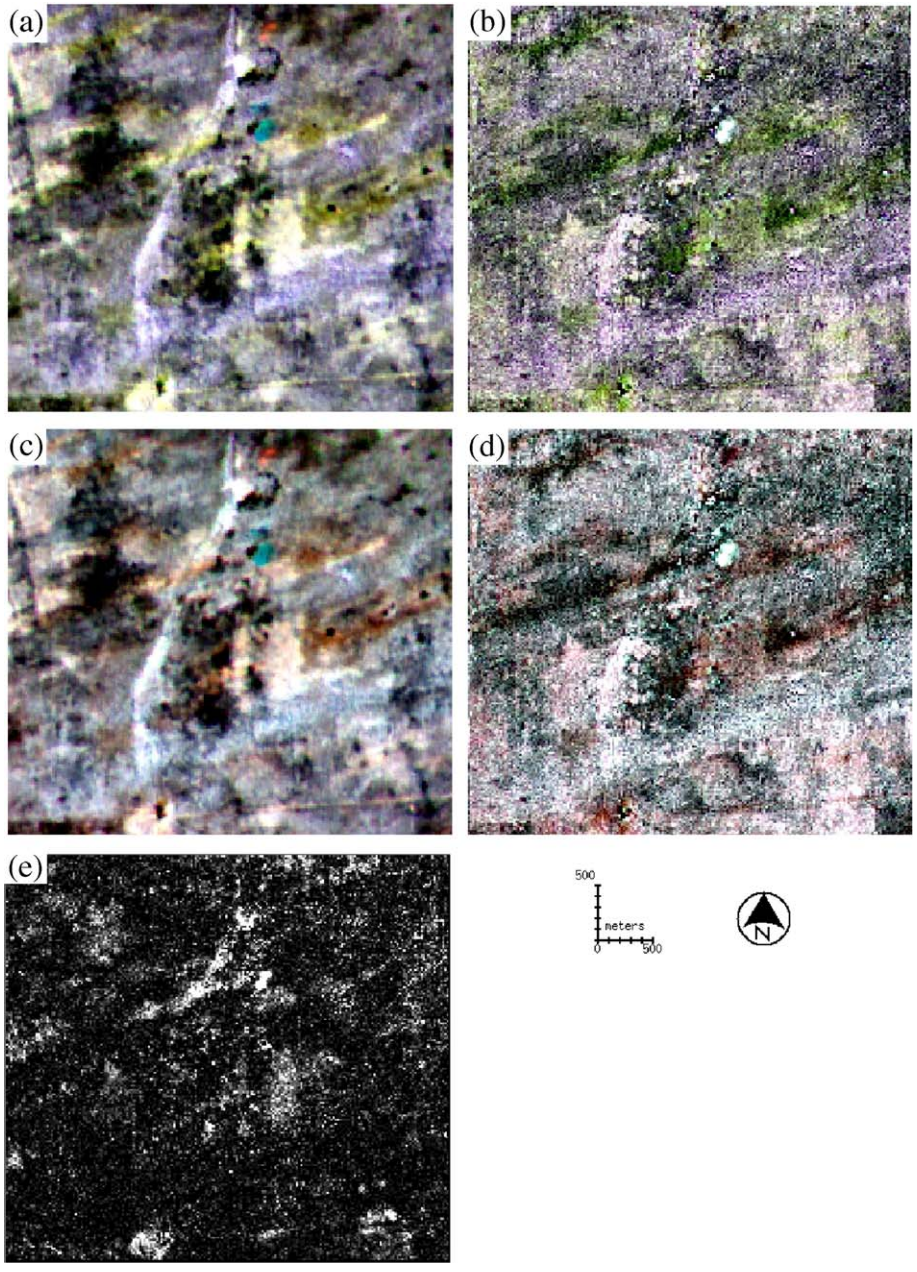

Fig. 9. Angular composites (a) CHRIS band 421, (b) band 421 simulation, (c) CHRIS band 431 composite, (d) band 431 simulation, (e) distribution of RMSE (range: 0.0 to 0.05). Note: scaling is 2-standard deviations on a per-band basis and is not consistent across images. Bands are ordered sequentially as in Fig. 2. The CHRIS composites (a) and (c) also provide an indication of the information content of multi-angle imagery.

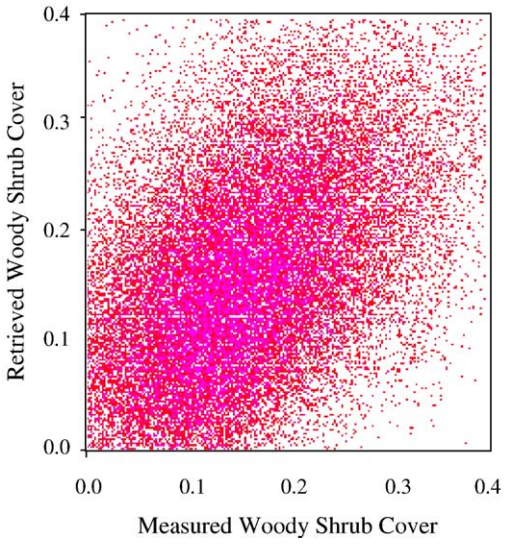

Fig. 10. Woody shrub cover obtained by inverting SGM with numerical methods on the entire CHRIS multi-angle red band subset (38,934 pixels) plotted against cover estimated from IKONOS panchromatic imagery. N=38,934, R^2=0.25, adjusted R^2=0.75, linear fit: y=0.447x+0.0571, RMSE=0.06. Mean RMSE on model fitting=0.002.

of the error terms. No constraints were imposed on retrieved values. Only mean shrub radius was left as a free parameter with other parameters set to typical values (b/r=0.2, h/b=2.0, crown leaf area index=2.08). Retrievals were thus effectively for woody shrub fractional cover, a function of shrub number density and mean radius. The plant shape parameter b/r was fixed at 0.2 (very oblate) and the crown center height parameter h/b was fixed at 2.00 m (low). This latter choice reflects the fact that honey mesquite crowns are not significantly raised from the surface on trunks, unlike trees. The leaf area index parameter is here applicable only to the upper canopy and was thus set to a typical mesquite leaf area index of 2.08 after White et al. (2000). Inversions were restricted to using only the 631 nm band images because in these wavelengths absorption by plant photosynthetic materials and pigments is maximum (and so contrast between soil and shrub crowns is maximum) and the single scattering approximation is more valid than in the near-infrared. This approach is supported by (Pinty et al., 2002) which asserts that the wavelength should be chosen to maximize the reflectance/absorption contrasts between vertically clumped elements and the background. Furthermore, Qin and Gerstl (2000) point out that the linear mixture assumption underlying geometric-optical models is more valid for the red than near infra-red wavelengths in arid environments; and BRDF model inversion experiments using numerical methods show that there are generally fewer problems such as trapping at local minima in the red compared to the NIR (Gemmell, 2000).

3. Results and discussion

The simulated CHRIS multi-angle reflectance values show a reasonable relation to the original CHRIS values in absolute terms, with some scatter owing to uncertainties in both the estimated background response and the upper canopy statistics (Fig. 8). In the spatial domain, modeled angular color composites demonstrate broadly similar distributions to those of the observed CHRIS images but with much greater noise, as expected (Fig. 9). The spatial distribution of error is not random but exhibits a marked increase – albeit to a maximum of ~0.07 with histogram tails close to zero at ~0.002 – over brighter areas with greater proportions of exposed soil; e.g., the area surrounding the West Well in the southern part of the SW quadrant, which is a location where livestock are watered. However, there are also locations where modeling error is greater over darker regions, as in the NE quadrant.

The inversion of the SGM against the multi-angle CHRIS data for fractional shrub cover resulted in a reasonable match with values estimated from IKONOS imagery, with a large spread that mainly reflects error in estimating the background contribution (Fig. 10). The mean absolute RMSE was 0.06 (n=38,934). A small proportion (2672/38,934=6.9%) of minimizations could not be completed satisfactorily: a solution was not found after the maximum number of iterations. The match between the multi-angle patterns and the model was for the vast majority of cases extremely good, with r^2 values of 0.95 and above (but recall that n=4, so the statistic may be misleading). The cumulative distribution of absolute error shows that about 80% of estimates are associated with a deviation from the IKONOS-estimated value of less than 0.08 (Fig. 11). The mapped values of retrieved fractional woody shrub cover show a notable similarity to the distribution of the IKONOS-estimated values (Fig. 12(a)–(b)). The distribution of absolute RMSE indicates areas where the retrieve cover values diverged from the measured values but show little correlation with the spatial arrangement; that is, while the retrieved cover values may differ importantly from the reference value, this is usually not important enough to disrupt the spatial composition of the map. There are some glaring inaccuracies in the retrieved

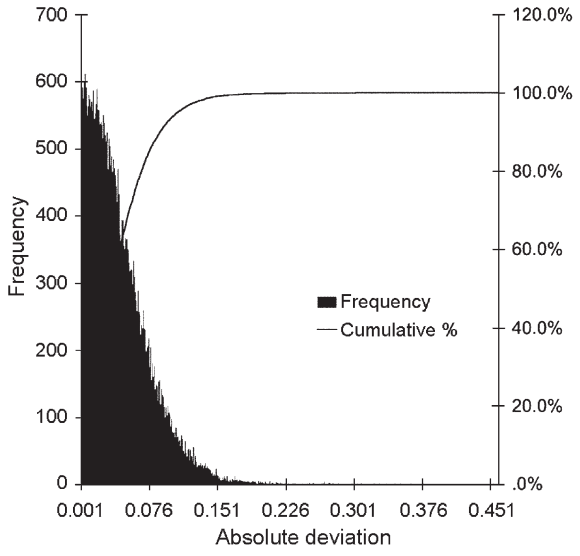

Fig. 11. Frequency distributions of absolute deviation between retrieved (SGM with calibrated Walthall soil–understory response) and measured woody shrub cover.

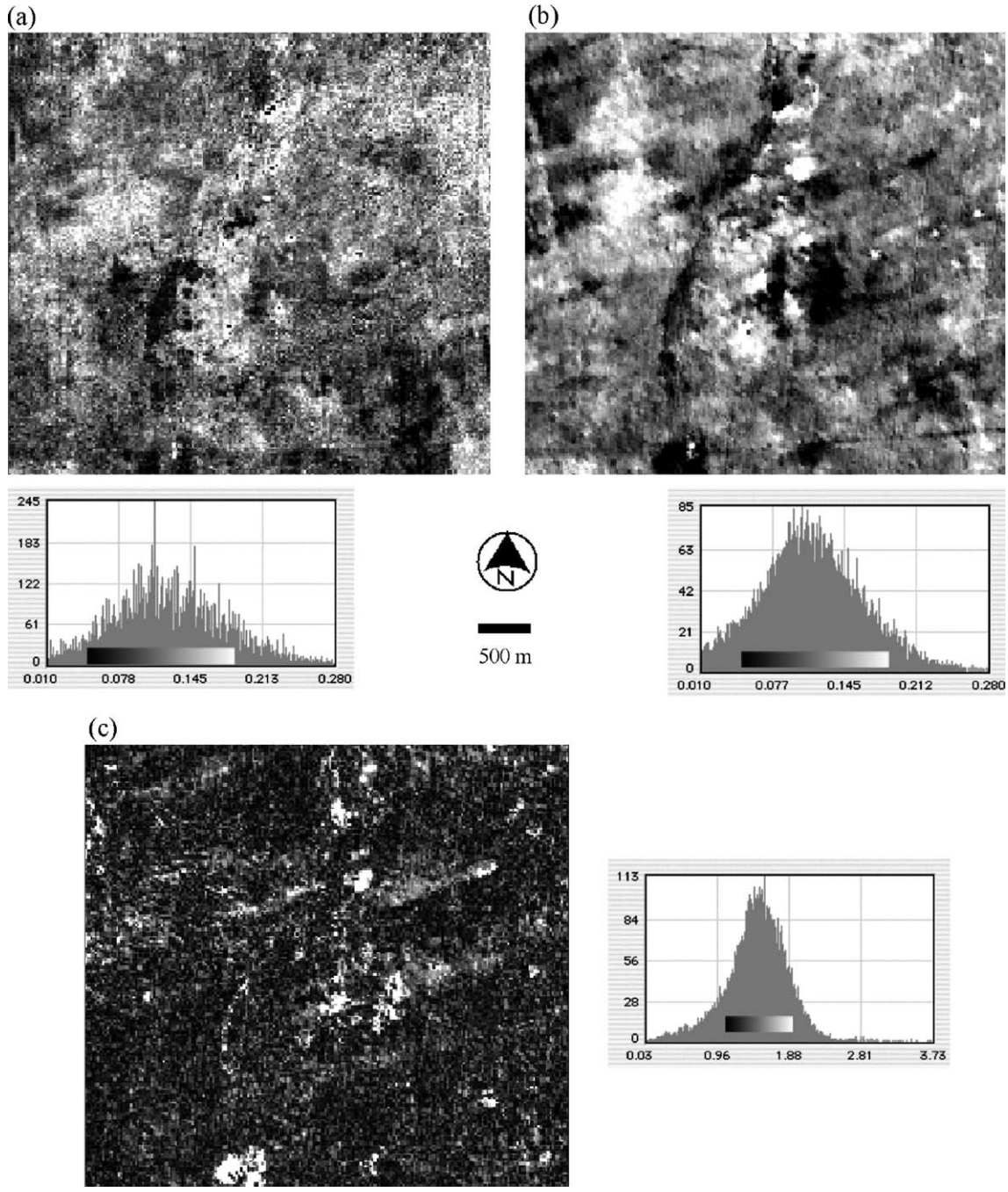

Fig. 12. (a) Fractional woody shrub cover estimated using IKONOS 1 m panchromatic imagery, (b) map of fractional woody shrub cover retrieved by adjusting the SGM against CHRIS 631 nm multi-angle data, (c) distribution of absolute root mean square error.

map, for example in a large area in the center where retrieved cover values were much lower than the reference values. These erroneous retrievals can usually be excluded on the basis that the values are close to zero: the map of zero or near-zero values (not shown) corresponds closely to the RMSE map. In addition, for much of this area the RMSE is high, providing an indication that there were problems fitting the model to the data. On the other hand, shrub cover was only slightly over-estimated in the grass-dominated area in the extreme southwestern part of the map, with no obvious change in error at the boundary with the shrub-dominated area to the north. The reference shrub cover map obtained by setting adaptive thresholds on subsets of the IKONOS panchromatic image is also subject to some level of uncertainty, although it is thought that this is not important at broad scales. A random sample of these estimates was compared to those obtained using QuickBird imagery and eCognition[1] segmentation software and a good but not excellent relation was found ($r^2 = 0.6$; Fig. 13). Thus it is likely that at

[1] Trade names included for the benefit of the reader and do not imply an endorsement of or a preference for the product listed by any of the institutions with which the authors are affiliated.

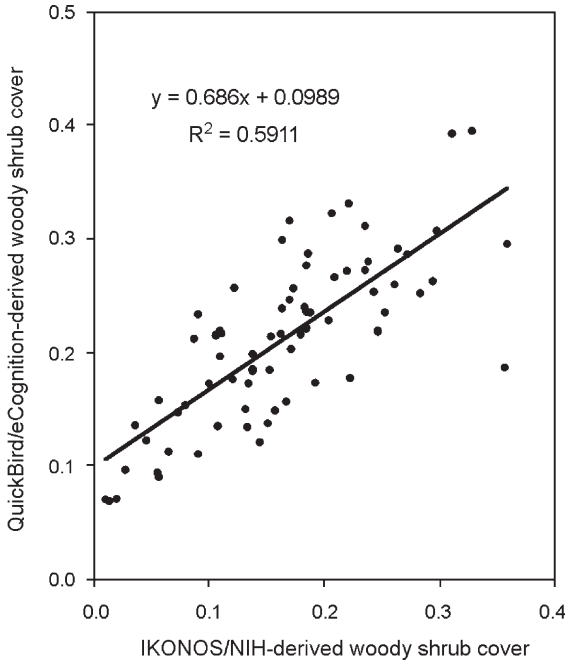

Fig. 13. The relationship between fractional woody shrub cover obtained using 1 m IKONOS panchromatic imagery and a thresholding algorithm and 0.6 m QuickBird panchromatic imagery using the eCognition segmentation algorithm (randomly selected test points).

least some of the discrepancies between retrieved and reference data sets are owing to error in the latter.

4. Conclusions

This study has reported on work aimed at determining the fractional cover of woody shrubs in desert grasslands in southern New Mexico at the landscape scale by exploiting the angular signature from CHRIS/Proba with a GO modeling approach, making some assumptions about the canopy and using the kernel weights of a Li–Ross model to obtain the background contribution (soil–understory brightness and anisotropy). The results show that the observed directional signal in the CHRIS geometries can be explained – with some error – in terms of the soil–understory background response and woody shrub cover. It also shows that maps of fractional woody shrub cover can be obtained – again, with some error – using these multi-angle data and modeling techniques. For this application the particular model used – SGM – provides one major advantage over the linear, semi-empirical, kernel-driven (LiSK) BRDF models adopted with great success for the MODIS BRDF/Albedo algorithm (Moody et al., 2005), or structural scattering indices (Gao et al., 2003): it provides surface parameters which are straightforward in their interpretation and validation. GO modeling is shown to be useful because it not only describes but also to some degree explains the observed remote sensing signal, particularly where multi-angle reflectance data sensitive to 3-D canopy structure are employed. It provides quantitative estimates of canopy parameters in a framework where the 3-D nature of the surface is handled explicitly, taking into account the shadowing effects that have often hounded nadir-only remote sensing approaches in arid environments.

CHRIS is a highly successful experimental sensor with a limited geographic coverage; the Jornada Experimental Range is 1 of the 22 core sites worldwide initially selected in 2000 prior to the launch of the Proba satellite. However the techniques developed here might well be used operationally over large areas with other kinds of remote sensing data which provide observations at multiple viewing and/or illumination angles: the NASA EOS Multi-angle Imaging SpectroRadiometer (MISR) is currently the best candidate since it provides radiance data at nine viewing angles with a 275 m ground sampling in the red channel. First attempts at applying these techniques with MISR data have been promising (Chopping et al., 2005). It is hoped that in the future GO models will benefit from increased coverage of the angular domain, especially if observations can be provided close to the solar principal plane where reflectance anisotropy is at a maximum, and/or for more than a single solar zenith angle. In this study, only four looks at a single moderate solar zenith angle and far from the principal plane were available to the SGM. The initial plans for CHRIS on Proba included use of the platform's agility to provide cross-track sampling (Cutter, 2002) but it remains to be seen whether this can be realized in practice. Without cross-track viewing the only way to extend the range of sun angles would be to combine data sets acquired at different times of the year but this is not feasible as surface conditions will be very different. Future work will pursue the retrieval of other important canopy structural parameters such as canopy height and shrub shape and determine whether it is possible to separate fractional cover into mean shrub radius and number density.

Acknowledgments

We would like to thank Evert Attema (European Space Agency), Michael Barnsley (University of Wales at Swansea), Mike Cutter and Sira Electro-Optics Ltd. (UK), the European Space Agency Proba Mission, Samantha Lavender (University of Plymouth), Kris Havstad and Connie Maxwell (USDA, ARS Jornada Experimental Range).

References

Asner, G. P., Borghi, C., & Ojeda, R. (2003). Desertification in Central Argentina: Regional changes in ecosystem carbon–nitrogen from imaging spectroscopy. *Ecological Applications*, *13*, 629−648.

Atjay, G. L., Ketner, P., & Duvigneaud, P. (1979). Terrestrial primary production and phytomass. In B. Bolin, E. T. Degens, S. Kempw, & P. Ketner (Eds.), *The global carbon cycle, SCOPE 13* (pp. 129−181). Chichester: John Wiley & Sons.

Bowyer, P., Danson, F. M., Trodd, N. M., & Dougill, A. J. (2001). Prospects for the remote sensing of savanna ve−getation using physically based plant canopy reflectance models. *Proc. Remote Sensing and Photogrammetry Society Annual General Meeting 2001* (pp. 241−245).

Calvão, T., & Palmeirim, J. M. (2004). Mapping Mediterranean scrub with satellite imagery: Biomass estimation and spectral behaviour. *International Journal of Remote Sensing*, *25*(16), 3113−3126.

Chen, J. M., Li, X., Nilson, T., & Strahler, A. (2000). Recent advances in geometrical optical modelling and its applications. *Remote Sensing Reviews*, *18*, 227−262.

Chopping, M., Laliberte, A., & Rango, A. (2004a). Exploitation of multi-angle data from CHRIS on Proba: First results from the Jornada Experimental Range, European Space Research Institute (ESRIN), Frascati, Italy, *ESA Special Publication SP-578*. Compiled by: H. Lacoste, ISBN No: 92-9092-889-1, 109–117.

Chopping, M., Su, L., Rango, A., & Maxwell, C. (2004b). Modelling the reflectance anisotropy of Chihuahuan Desert grass–shrub transition canopy–soil complexes. *International Journal of Remote Sensing*, *25*(14), 2725−2745.

Chopping, M., Martonchik, J. V., Rango, A., Peters, D. P. C., Su, L., & Laliberte, A. (2005). Geometric-optical modeling of desert grassland canopy structure with MISR. *Proceedings of The 9th International Symposium on Physical Measurements and Signature in Remote Sensing (ISPMSRS 2005), Beijing, Oct. 17–19, 2005International Society for Photogrammetry and Remote Sensing*, *vol. I* (pp. 141−143).

Chopping, M. J., Rango, A., Havstad, K. M., Schiebe, F. R., Ritchie, J. C., Schmugge, T. J., et al. (2003). Canopy attributes of Chihuahuan Desert grassland and transition communities derived from multi-angular 0.65 μm airborne imagery. *Remote Sensing of Environment*, *85*(3), 339−354.

Combal, B., Baret, F., Weiss, M., Trubuil, A., Macé, D., Pragnère, A., et al. (2002). Retrieval of canopy biophysical variables from bidirectional reflectance using prior information to solve the ill-posed inverse problem. *Remote Sensing of Environment*, *84*, 1−15.

Cutter, M. (2002). *CHRIS (Compact High Resolution Imaging Spectrometer), presentation at IGARSS'02, Toronto, Canada.*

European Space Agency Scientific Campaign Unit ESTEC. (1999). *Exploitation of CHRIS data from the Proba Mission for Science and Applications, Experimenters' Handbook Issue 4: Baseline Programme, ESA-ESTEC.*

Gao, F., Schaaf, C. B., Strahler, A. H., Jin, Y., & Li, X. (2003). Detecting vegetation structure using a kernel-based BRDF model. *Remote Sensing of Environment*, *86*(2), 198−205.

Gemmell, F. (2000). Testing the utility of multi-angle spectral data for reducing the effects of background spectral variations in forest reflectance model inversion. *Remote Sensing of Environment*, *72*, 46−63.

Gibbens, R. P., Beck, R. F., McNeely, R. P., & Herbel, C. H. (1992). Recent rates of mesquite establishment in the northern Chihuahuan Desert. *Journal of Range Management*, *45*, 585−588.

Huete, A. R. (1988). A soil-adjusted vegetation index (SAVI). *Remote Sensing of Environment*, *25*, 295−309.

Li, X., Gao, F., Wang, J., Strahler, A., Lucht, W., & Schaaf, C. (2002). Parameter error propagation in BRDF derived by fitting multiple angular observations at a single sun position. *Proc. IGARSS 2002* (pp. 3142−3144).

Li, X., & Strahler, A. H. (1992). Geometric-optical bidirectional reflectance modeling of the discrete crown vegetation canopy: Effect of crown shape and mutual shadowing. *IEEE Transactions on Geoscience and Remote Sensing*, *30*(2), 276−291.

Moody, E. G., King, M. D., Platnick, S., Schaaf, C. B., & Gao, F. (2005). Spatially complete global spectral surface albedos: Value-added datasets derived from Terra MODIS land products. *IEEE Transactions on Geoscience and Remote Sensing*, *43*, 144−158.

Ni, W., & Li, X. (2000). A coupled vegetation–soil bidirectional reflectance model for a semi-arid landscape. *Remote Sensing of Environment*, *74*(1), 113−124.

Okin, G. S., Roberts, D. A., Murray, B., & Okin, W. J. (2001). Practical limits on hyperspectral vegetation discrimination in arid and semiarid environments. *Remote Sensing of Environment*, *77*, 212−225.

Peters, D. P. C., & Herrick, J. E. (2001). Modelling vegetation change and land degradation in semiarid and arid ecosystems: An integrated hierarchical approach. *Advances in Environmental Monitoring and Modelling*, *2*(1), 1−29.

Pilger, N., Peddle, D. R., & Luther, J. E. (2002). Estimation of forest cover type and structure from Landsat TM imagery using a canopy reflectance model for biomass mapping in Western Newfoundland. Proceedings of the International Geoscience and Remote Sensing Symposium 2002 (IGARSS '02)/24th Canadian Symposium on Remote Sensing, Toronto, Canada, 2002.

Pinty, B., Widlowski, J. -L., Gobron, N., Verstraete, M. M., & Diner, D. J. (2002). Uniqueness of multiangular measurements: Part 1. An indicator of subpixel surface heterogeneity from MISR. *IEEE Transactions on Geoscience and Remote Sensing*, *40*(7), 1560−1573.

Qi, J., Chehbouni, A., Huete, A. R., Kerr, Y. H., & Sorooshian, S. (1994). A modified soil adjusted vegetation index: MSAVI. *Remote Sensing of Environment*, *48*, 119−126.

Qin, W., & Gerstl, S. A. W. (2000). 3-D scene modeling of Jornada semi-desert vegetation cover and its radiation regime. *Remote Sensing of Environment*, *74*, 145−162.

Rahman, A. F., & Gamon, J. A. (2004). Detecting biophysical properties of a semi-arid grassland and distinguishing burned from unburned areas with hyperspectral reflectance. *Journal of Arid Environments*, *58*, 597−610.

Rango, A., Ritchie, J. C., Kustas, W. P., Schmugge, T. J., & Havstad, K. M. (1998). JORNEX: Remote sensing to quantify long-term vegetation change and hydrological fluxes in an arid rangeland environment. In H. Wheater, & C. Kirby (Eds.), *Hydrology in a changing environment* (pp. 585−590). London: John Wiley.

Ray, T. (1995). *Remote Monitoring of Land Degradation in Arid/Semiarid Regions*, Unpublished Ph.D. Dissertation, Division of Geological and Planetary Sciences, California Institute of Technology, Pasadena, CA.

Ross, J. K. (1981). *The radiation regime and architecture of plant stands.* The Hague: Dr. W. Junk Publishers 392 pp.

Scarth, P., & Phinn, S. (2000). Determining forest structural attributes using an inverted geometric-optical model in mixed eucalypt forests, Southeast Queensland, Australia. *Remote Sensing of Environment*, *71*, 141−157.

Schaaf, C. B., Li, X., & Strahler, A. H. (1995). Using a geometric-optical model to calculate the bidirectional and hemispherical reflectance of forested slopes. *Proceedings of SPIE (Multispectral and Microwave Sensing of Forestry, Hydrology, and Natural Resources)*, *vol. 2314* (pp. 21−26).

Vermote, E., Tanre, D., Deuze, J. L., Herman, M., & Morcrette, J. J. (1997). Second Simulation of the Satellite Signal in the Solar Spectrum, (6S): An overview. *IEEE Transactions on Geoscience and Remote Sensing*, *35*(3), 675−686.

Walthall, C. L., Norman, J. M., Welles, J. M., Campbell, G., & Blad, B. L. (1985). Simple equation to approximate the bidirectional reflectance from vegetative canopies and bare surfaces. *Applied Optics*, *24*(3), 383−387.

Wanner, W., Li, X., & Strahler, A. H. (1995). On the derivation of kernels for kernel-driven models of bidirectional reflectance. *Journal of Geophysical Research*, *100*, 21077−21090.

Weiss, M., Myneni, F., Pragnère, R. B., & Knyazikhin, A. (2000). Investigation of a model inversion technique to estimate canopy biophysical variables from spectral and directional reflectance data. *Agronomie*, *20*, 3−22.

White, M. A., Asner, G. P., Nemani, R. R., Privette, J. L., & Running, S. W. (2000). Measuring fractional cover and leaf area index in arid ecosystems — digital camera, radiation transmittance, and laser altimetry methods. *Remote Sensing of Environment*, *74*(1), 45−57.